







ARTICLE OPEN ACCESS

Use of Whole Cells and Cell-Free Extracts of Catalase-Deficient *E. coli* for Peroxygenase-Catalyzed Reactions

Ana C. Ebrecht¹  | U. Joost Luelf²  | Kamini Govender¹  | Diederik J. Opperman¹  | Vlada B. Urlacher²  | Martha S. Smit¹ 

¹Department of Microbiology and Biochemistry, University of the Free State, Bloemfontein, South Africa | ²Institute of Biochemistry, Heinrich Heine University Düsseldorf, Düsseldorf, Germany

Correspondence: Martha S. Smit (smitms@ufs.ac.za)

Received: 15 October 2024 | **Revised:** 4 February 2025 | **Accepted:** 15 February 2025

Funding: This work was supported by the South African Council for Scientific and Industrial Research—Industrial Biocatalysis Hub (CSIR-IBH) initiative funded by the South African Department of Science and Innovation (DSI) and the Technology Innovation Agency (TIA).

Keywords: catalase-deficient *E. coli* | epoxidation | hydrogen peroxide | hydroxylation | peroxygenase | sulfoxidation

ABSTRACT

Unspecific peroxygenases (UPOs) and cytochrome P450 monooxygenases (CYPs) with peroxygenase activity are becoming the preferred biocatalysts for oxyfunctionalization reactions. While whole cells (WCs) or cell-free extracts (CFEs) of *Escherichia coli* are often preferred for cofactor-dependent monooxygenase reactions, hydrogen peroxide (H₂O₂) driven peroxygenase reactions are generally performed with purified enzymes, because the catalases produced by *E. coli* are expected to quickly degrade H₂O₂. We used the CRISPR/Cas system to delete the catalase encoding chromosomal genes, *katG*, and *katE*, from *E. coli* BL21-Gold (DE3) to obtain a catalase-deficient strain. A short UPO, *DcaUPO*, and two CYP peroxygenases, *SscaCYP_E284A* and *CYP102A1_21B3*, were used to compare the strains for peroxygenase expression and subsequent sulfoxidation, epoxidation, and benzylic hydroxylation activity. While 10 mM H₂O₂ was depleted within 10 min after addition to WCs and CFEs of the wild-type strain, at least 60% remained after 24 h in WCs and CFEs of the catalase-deficient strain. CYP peroxygenase reactions, with generally lower turnover frequencies, benefited the most from the use of the catalase-deficient strain. Comparison of purified peroxygenases in buffer versus CFEs of the catalase-deficient strain revealed that the peroxygenases in CFEs generally performed as well as the purified proteins. We also used WCs from catalase-deficient *E. coli* to screen three CYP peroxygenases, wild-type *SscaCYP*, *SscaCYP_E284A*, and *SscaCYP_E284I* for activity against 10 substrates comparing H₂O₂ consumption with substrate consumption and product formation. Finally, the enzyme-substrate pair with highest activity, *SscaCYP_E284I*, and *trans*- β -methylstyrene, were used in a preparative scale reaction with catalase-deficient WCs. Use of WCs or CFEs from catalase-deficient *E. coli* instead of purified enzymes can greatly benefit the high-throughput screening of enzyme or substrate libraries for peroxygenase activity, while they can also be used for preparative scale reactions.

1 | Introduction

Unspecific peroxygenases (UPOs) and cytochrome P450 monooxygenases (CYPs) with peroxygenase activity are becoming the preferred catalysts for reactions traditionally performed with monooxygenases (Monterrey et al. 2023; Xu et al. 2023). While

whole cells (WCs) or cell-free extracts (CFEs) of *Escherichia coli* are often preferred for monooxygenase-catalyzed reactions which require reduced cofactors and their regeneration, hydrogen peroxide (H₂O₂) driven peroxygenase reactions are generally performed with purified enzymes, since it is assumed that the catalases produced by *E. coli* will quickly catalyze the disproportionation of H₂O₂. Two

This is an open access article under the terms of the [Creative Commons Attribution-NonCommercial-NoDerivs](https://creativecommons.org/licenses/by-nc-nd/4.0/) License, which permits use and distribution in any medium, provided the original work is properly cited, the use is non-commercial and no modifications or adaptations are made.

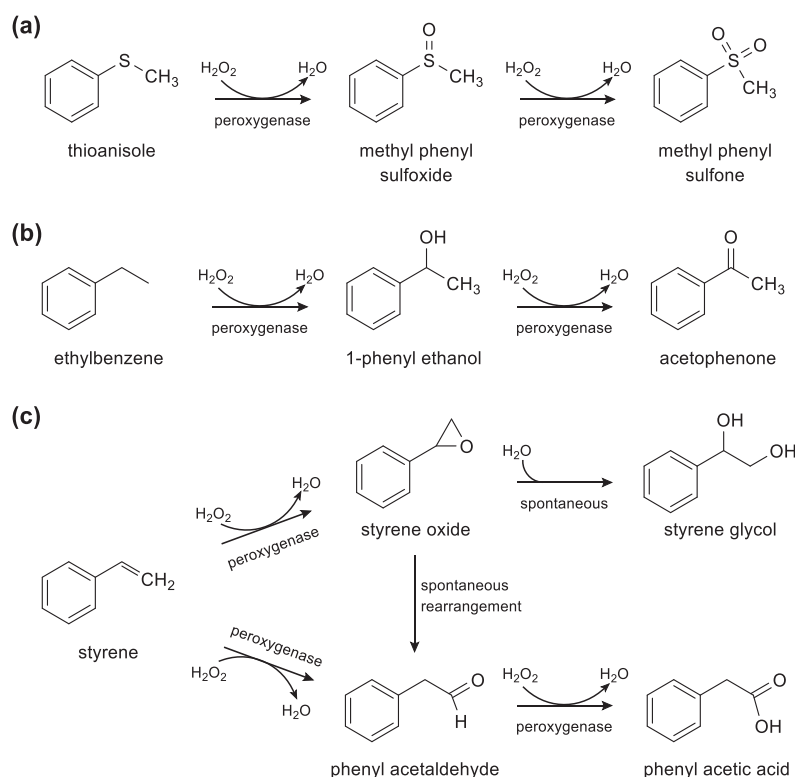
© 2025 The Author(s). *Biotechnology and Bioengineering* published by Wiley Periodicals LLC.

catalases (*katG* and *katE*), together with an alkyl hydroperoxide reductase (*AhP*) are responsible for scavenging H_2O_2 in *E. coli* with the catalases dominating when H_2O_2 levels exceed $20\ \mu\text{M}$ (Xu et al. 2020; Liu et al. 2021). In the case of UPOs, *Pichia pastoris* is the preferred host for heterologous expression because these are extracellular glycosylated fungal enzymes that generally do not express well in *E. coli* (Kinner et al. 2021, Monterrey et al. 2023). However, *E. coli* is gradually more often used for the expression of short UPOs (Linde et al. 2020, Kinner et al. 2021), and recently a superfolder-green-fluorescent-protein (sfGFP) mediated secretion system was developed that facilitated the expression of four different UPOs, including the long UPO, *AaeUPO*, in *E. coli* (Yan et al. 2024). The activity of these UPOs displayed on the cell surface of *E. coli* was detected using WCs and CFEs of *E. coli* BL21(DE3), despite possible disproportionation of H_2O_2 by the well-described catalases of *E. coli*.

Catalase-deficient strains of *E. coli* have been constructed and characterized (Nakagawa et al. 1996; Hui et al. 2014; Xu et al. 2020; Liu et al. 2021). Nakagawa et al. (1996) constructed a catalase-deficient strain of *E. coli* for the large-scale production of catalase-free uricase preparations. They found that deletion of both chromosomal genes, *katG*, and *katE*, from a strain derived from *E. coli* K-12 did not affect growth or uricase production. The same catalase-deficient *E. coli* strain was subsequently used by the Arnold group to develop variants of CYP102A1 with peroxygenase activity (Cirino and Arnold 2002, 2003; Salazar et al. 2003). More recently Xu et al. (2020) deleted *katG* and *katE* from *E. coli* BL21 (DE3), the commercially available B strain commonly used for heterologous protein expression. They used this catalase-deficient *E. coli* strain to

develop a high-throughput screening method relying on H_2O_2 consumption detected by the colorimetric Amplex Red assay. This screening method was used to screen large DNA shuffling and random mutagenesis libraries of the fatty acid decarboxylases OleTJE (CYP152L1) and CYP-Sm46Δ29 (CYP152L2) for improved variants (Xu et al. 2020).

We deleted *katG* and *katE* from *E. coli* BL21-Gold(DE3), to investigate the use of WCs and CFEs from catalase-deficient strains expressing different known peroxygenases for different hydrogen peroxide driven reactions. Three heme-thiolate-based peroxygenases were selected, namely *DcaUPO*, a short UPO from *Daldinia caldariorum* (Linde et al. 2020), *SscaCYP_E284A*, a variant of *SscaCYP* a CYP peroxygenase from *Streptomyces scabiei* which contains an Asp instead of the usual Thr in the I helix, both previously described by our group (Ebrecht et al. 2023), and the CYP102A1_21B3 CYP peroxygenase developed by the Arnold group from the N-terminal heme-domain of CYP102A1 (Cirino and Arnold 2003). Three reactions which all three enzymes can catalyze to various degrees were selected to evaluate peroxygenase activity using WCs and CFEs. These were sulfoxidation of thioanisole, benzylic hydroxylation of ethylbenzene, and conversion, mainly epoxidation, of styrene (Scheme 1). Next, we evaluated the robustness of the colorimetric H_2O_2 consumption assay by screening the wild-type *SscaCYP*, together with two mutants, *SscaCYP_E284A* used above and *SscaCYP_E284I* also previously described by us (Ebrecht et al. 2023), for activity against 10 different substrates. From this screening, we finally selected the enzyme-substrate pair with highest activity, *SscaCYP_E284I*, and *trans*- β -



SCHEME 1 | Reactions used for comparing activities were (a) sulfoxidation of thioanisole to methyl phenyl sulfoxide, (b) hydroxylation of ethylbenzene to 1-phenyl ethanol and further to acetophenone, and (c) epoxidation or anti-Markovnikov type oxidation of styrene to styrene oxide and phenylacetaldehyde, respectively. Methyl phenyl sulfone, 1-phenyl ethanol, and phenylacetaldehyde can be further oxidized in a second round of peroxygenase reactions. Phenylacetaldehyde might also be formed by rearrangement of styrene oxide (Aschenbrenner et al. 2024).

methylstyrene, for a preparative scale reaction using catalase-deficient WCs.

2 | Results and Discussion

CRISPR/Cas-assisted λ -red recombineering was used for successive in-frame deletions of the *katE* and *katG* genes in *E. coli* BL21-Gold(DE3). Successful knockout mutants were identified using colony PCR and verified by Sanger sequencing. Deletion of the catalase-encoding genes was further confirmed by monitoring the fate of H_2O_2 (10 mM) added to WCs and CFEs of wild-type *E. coli* BL21-Gold(DE3) (WT) and its catalase-deficient derivative (CD), both transformed with empty pET-28a (+). As expected, H_2O_2 was quickly depleted by catalase-containing WCs and CFEs from the catalase-containing *E. coli*, with no H_2O_2 left after 20 min (Figure 1a). However, H_2O_2

levels dropped slowly in WCs and CFEs from the catalase-deficient strain, with more than 5 mM left after 8 h which remained up to 24 h. Xu et al. (2020) also observed H_2O_2 consumption (ca. 20%) in their catalase-deficient strain with *katE* and *katG* genes deleted and ascribed it to the activity of the alkyl hydroperoxide reductase (AhP) which functions at low H_2O_2 concentrations ($< 10 \mu\text{M}$) or other unknown scavenging enzymes. In their experience a triple deletion strain with the *ahp* gene also deleted displayed severe growth defects. After 8 h H_2O_2 stability was similar to what we observed in buffer without WCs or CFEs, where 7 mM H_2O_2 remained after 24 h.

The catalase-deficient strain displayed satisfactory growth and enzyme production. Biomass harvested from its cultures expressing the different peroxygenases was 6%–18% less than from wild-type cultures (Figure 1b). *DcaUPO* and *SscaCYP_E284A* expressed equally well in both catalase-deficient and wild-type strains, while expression of CYP102A1_21B3 was lower in the catalase-deficient strain (Figure 1c).

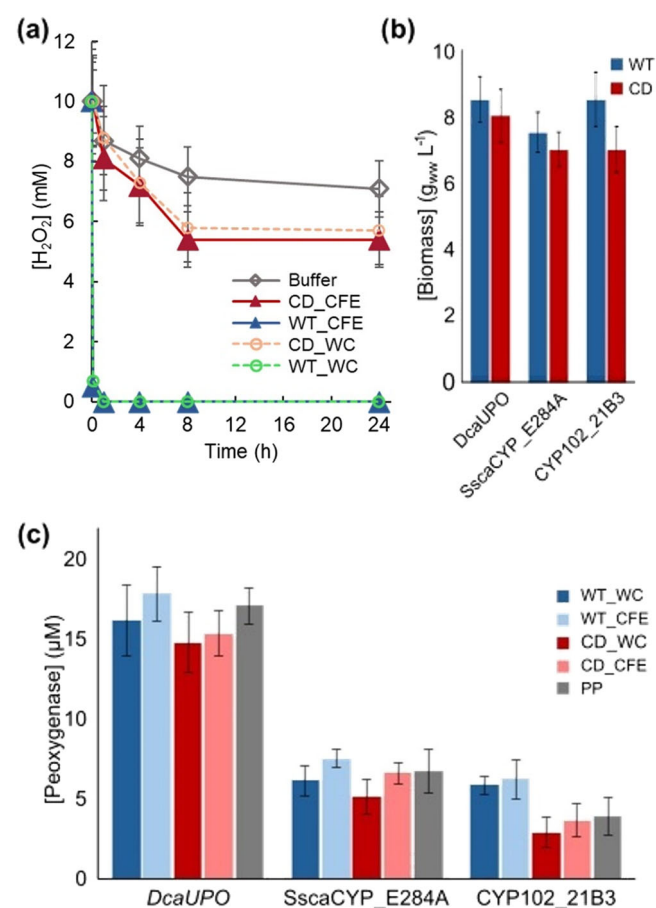


FIGURE 1 | (a) Stability of H_2O_2 (10 mM) in buffer containing WCs (0.1 g wet weight mL^{-1}) (open circles) or CFEs (produced after cell disruption at 0.1 g wet weight mL^{-1}) (closed triangles) from wild-type (WT) and catalase-deficient (CD) *E. coli* and in buffer without WCs or CFEs (gray open diamonds) at 25°C, pH7. (b) Biomass (wet weight) recovered from cultures of WT and CD *E. coli* when cells were harvested for biotransformations. (c) Concentrations of different peroxygenases (based on CO difference spectra) in biotransformation reactions containing WCs (dark colors) or CFEs (light colors) from WT (blue) and CD (red) *E. coli* (0.1 g wet weight mL^{-1}) as well as purified protein (grey). Averages and standard deviations were calculated from at least three independent repeats.

Given how quickly H_2O_2 is depleted by catalase-containing WCs and CFEs, it was surprising that in 24 h reactions, sulfoxidation of thioanisole by all three peroxygenases could be detected with WCs and CFEs of the wild-type strain even when H_2O_2 (20 mM) was added in a single dose to start reactions (Figure 2a). The initial sulfoxidation of thioanisole by *DcaUPO* is evidently a very fast reaction since there was essentially no difference between reactions with catalase-containing and catalase-deficient CFEs both giving approximately 80% conversion of the substrate. WC sulfoxidation by *DcaUPO* benefited from the use of catalase-deficient cells, most likely because H_2O_2 diffusion into the cells is quicker than thioanisole diffusion. When H_2O_2 was produced in situ by glucose oxidation with glucose oxidase (GOx) there was a significant difference in the product distribution from catalase-containing and catalase-deficient CFEs, with further oxidation of the sulfoxide to sulfone by *DcaUPO* more prevalent in catalase-deficient CFEs (Figure 2a). In the case of *SscaCYP_E284A*, which was expressed at lower concentrations, there was a clear benefit to using the catalase-deficient strain, whether H_2O_2 was added in a single dose or produced in situ by GOx. With catalase-deficient WCs and CFEs, however, significant sulfoxidation to the sulfone was observed. Chiral analysis of extracts from reactions with catalase-deficient WCs and CFEs containing *SscaCYP_E284A* revealed that use of WCs or CFEs did not reduce enantioselectivity when compared with previous results obtained with purified protein when the (*S*)-enantiomer of the sulfoxide was produced with 81% *ee* (Ebrecht et al. 2023) (Figure S7). Activity of CYP102A1_21B3 towards thioanisole was much lower than that of the other two enzymes, with only traces of sulfoxide observed with wild-type WCs and CFEs. Highest conversions were achieved when H_2O_2 was supplied in situ by GOx. However, no further oxidation to the sulfone was observed with CYP102A1_21B3 (Figure 2a).

All three peroxygenases displayed lower activity toward ethylbenzene than to thioanisole. *SscaCYP_E284A* displayed barely detectable activity with wild-type and catalase-deficient CFEs only when H_2O_2 was supplied in situ by GOx (Figure 2b). In *DcaUPO*-catalyzed reactions activity was low with WCs in both strains. In similar CFE reactions with H_2O_2 also added as a single dose,

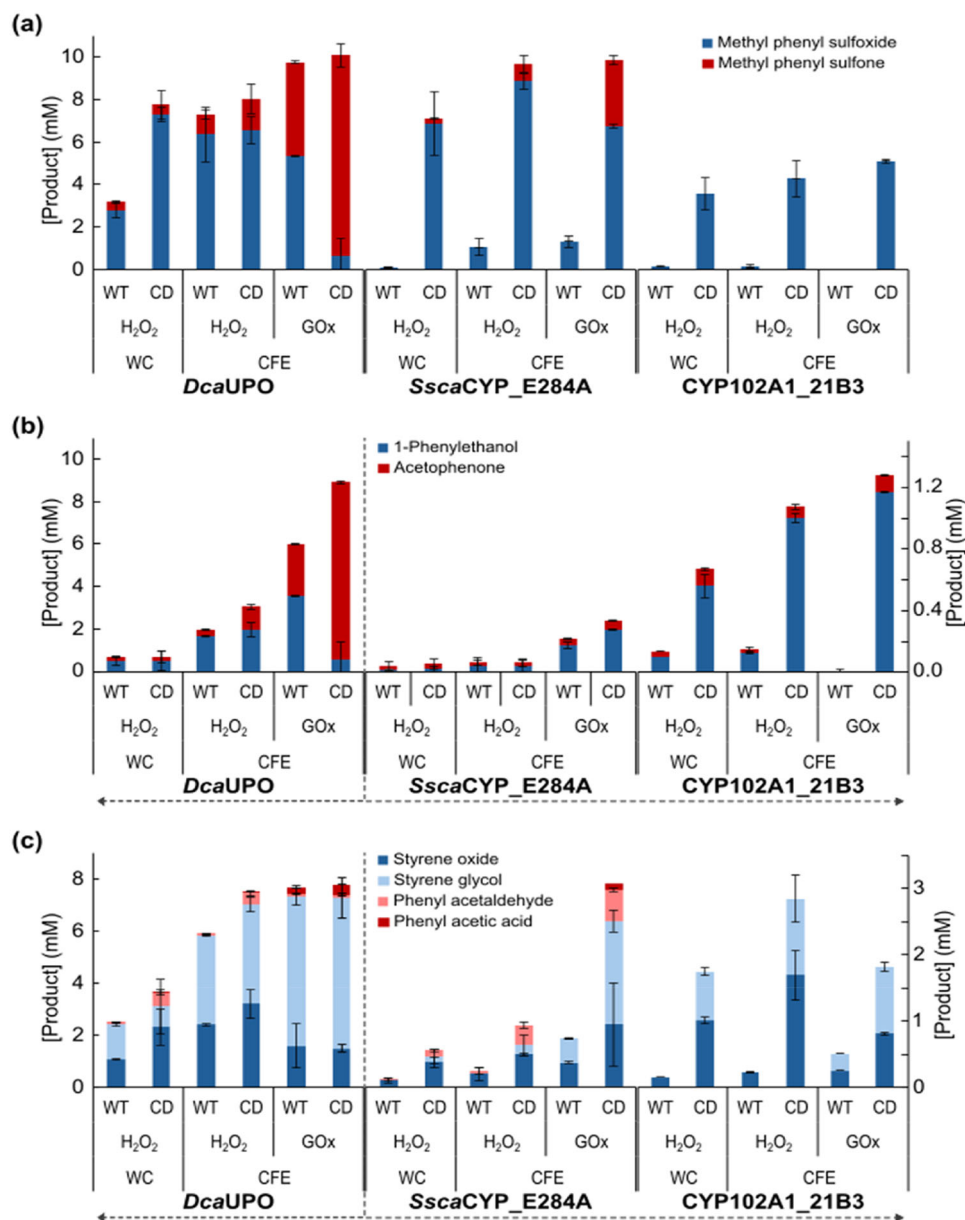


FIGURE 2 | Concentrations of different products formed by *DcaUPO*, *SscaCYP_E284A*, and *CYP102A1_21B3* from (a) thioanisole, (b) ethylbenzene and (c) styrene in 24 h reactions using WCs or CFEs of wild-type (WT) and catalase-deficient (CD) *E. coli*. H₂O₂ was added in a single dose to start reactions or H₂O₂ was produced in situ by oxidation of glucose with GOx. Concentrations of products from thioanisole are displayed by the axis on the left. Arrows point to products formed by *DcaUPO* from ethylbenzene and styrene displayed by the axis on the left and those from ethylbenzene and styrene produced by *SscaCYP_E284A* and *CYP102A1_21B3* by the axis on the right. Reactions contained WCs or CFEs of WT and CD *E. coli* (0.1 g wet weight mL⁻¹), substrate (10 mM), acetone (5% (v/v)), H₂O₂ (20 mM) or GOx (0.2 U mL⁻¹) with glucose (100 mM). Averages and standard deviations were calculated from at least three independent reactions.

activity in catalase-deficient CFEs was higher with more of the initially formed 1-phenyl ethanol further oxidized to acetophenone. When H₂O₂ was supplied in situ by GOx the advantage to using catalase-deficient CFEs became even more apparent with ca. 80% of ethylbenzene hydroxylated and subsequently oxidized to acetophenone while with wild-type CFEs ca. 60% was hydroxylated with only ca. 24% further oxidized to acetophenone. Activity of *CYP102A1_21B3* toward ethylbenzene was much lower than that of *DcaUPO* with in the best reactions only ca. 10% conversion and very little oxidation to acetophenone. However, activities with both WCs and CFEs were significantly improved when the catalase-deficient strain was used (Figure 2b).

Oxidation of styrene by these peroxygenases yielded mainly styrene oxide which was in 24 h reactions spontaneously hydrolyzed to styrene glycol. In the case of *DcaUPO*, which again yielded the most product given its high concentration, small amounts of phenylacetaldehyde were also detected, some of which were oxidized to phenylacetic acid (Figure 1c). In these reactions, activity was only slightly improved when catalase-deficient WCs and CFEs were used with H₂O₂ added in a single dose. With in situ generation of H₂O₂ by GOx there was in 24 h reactions, no benefit to using catalase-deficient CFEs. *CYP102A1_21B3* and *SscaCYP_E284A* activities in all cases benefited significantly from the use of the catalase-deficient

strain. *SscaCYP_E284A* produced relatively more phenylacetaldehyde than the other two peroxygenases.

Next, we compared the performance of purified peroxygenases in buffer and peroxygenases in CFEs of catalase-deficient *E. coli* in a series of time-course experiments. In these experiments, H_2O_2 was added as a single dose or produced in situ using either GOx or formate oxidase (FOx). A total number of oxygenations was calculated and plotted assuming that the formation of sulfone from thioanisole, acetophenone from ethylbenzene, and phenylacetic acid from phenylacetaldehyde required in each case two sequential peroxygenase reactions rather than peroxidase activity (Figure S1). These values were used to calculate turnover numbers (TONs) at the times when reactions leveled off (Figure 3, Table S3). It is evident from these results that the peroxygenases in CFEs of the catalase-deficient strain generally performed at least as well as the purified peroxygenases in buffer. The exception was the purified *DcaUPO* which, when H_2O_2 was produced in situ, achieved maximum product concentrations already after 8 h in thioanisole and ethylbenzene conversions, while these reactions with CFE took 24 h (Figure S1, Table S3). This might be due to the GOx and FOx being unable to supply sufficient H_2O_2 quickly enough for the high concentration of *DcaUPO* when enzymes in the CFEs consumed some of the H_2O_2 , glucose and/or formate. On the other hand, in the case of CYP102A1_21B3, which displayed low activity on all substrates, the CFEs generally yielded better results than the purified peroxygenases, possibly because the CFEs improved stability of the CYP102A1_21B3. Notable from these time course experiments are the reactions with styrene which in all cases with all three enzymes leveled off within 2 h, indicating that styrene most likely inhibited or denatured these peroxygenases. Activity of *SscaCYP_E284A* toward ethylbenzene, in all cases, ceased within 1 h.

Xu et al. (2020) used CFEs of catalase-deficient *E. coli* in the H_2O_2 -dependent high throughput screening method they had used to screen libraries derived from OleT_{JE} (CYP152L1) and CYP-Sm46Δ29 (CYP152L2) for decarboxylase activity against lauric acid. We explored whether WCs of catalase-deficient *E. coli* can similarly be used by screening *SscaCYP_E284A* as well as WT *SscaCYP* and a second mutant *SscaCYP_E284I* for activity against 10 different substrates (Figure S8). Although H_2O_2 consumption could reliably be detected in WC assays, the correlation between H_2O_2 consumption and activity detected with GC analysis (substrate consumption and product formation) was evidently influenced by the enzymes and substrates (Figure 4). H_2O_2 consumption accurately indicated the activity of *SscaCYP_E284I* against *trans*-β-methylstyrene, α-methylstyrene, 4-methoxybenzyl alcohol, and vanillyl alcohol and the activity of *SscaCYP_E284A* against *trans*-β-methylstyrene. However, it did not indicate activity of *SscaCYP_E284I* against 1,5-cyclooctadiene and of *SscaCYP_E284A* against 4-methoxybenzyl alcohol, both for which products were detected with GC, or any activity against styrene, which all three enzymes converted. The presence of the CYPs in the absence of substrate increased H_2O_2 consumption in an enzyme-dependent manner, with *SscaCYP_E284I* consuming at least 60% more H_2O_2 than the no-CYP control. In some instances, the presence of substrate reduced H_2O_2 consumption, particularly in the case of *SscaCYP_E284I* where propylbenzene, 3-methoxybenzyl

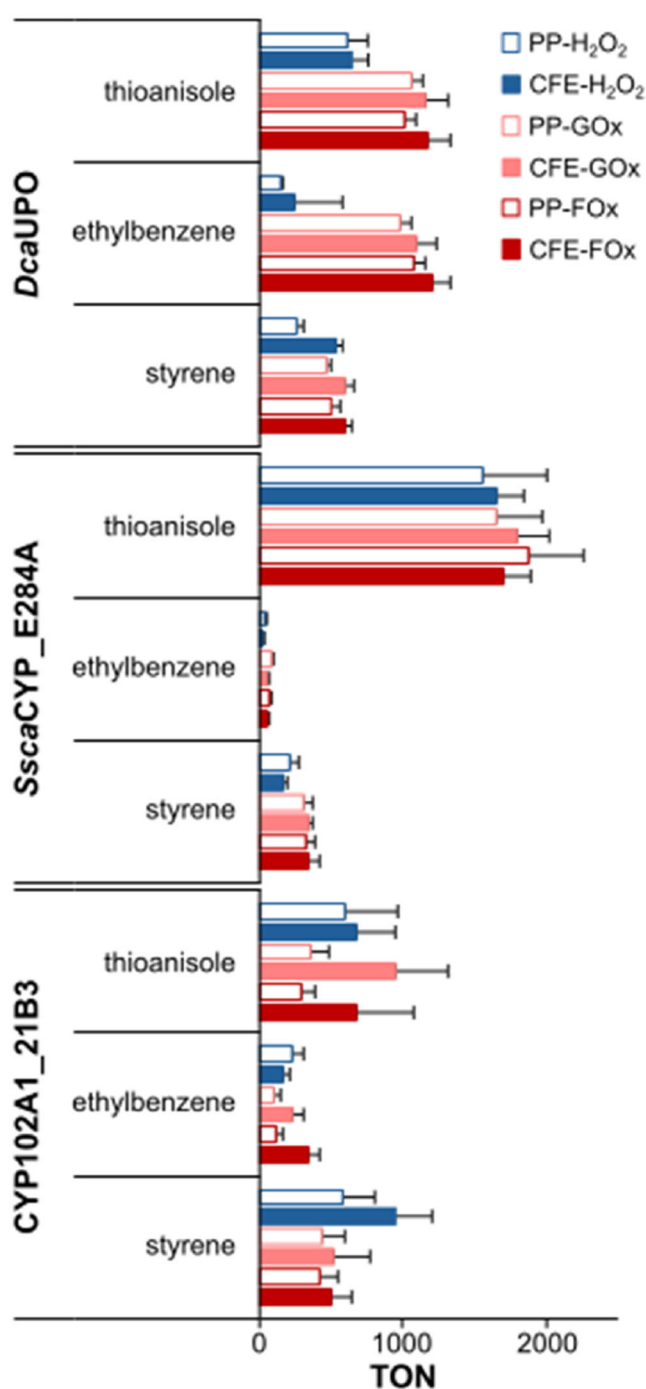


FIGURE 3 | Comparison of turnover numbers (TON) of *DcaUPO*, *SscaCYP_E284A*, and *CYP102A1_21B3* in CFEs of catalase-deficient *E. coli* and as purified protein. TONs were calculated from time course experiments at times when activities leveled off (Table S3, Figure S1). H_2O_2 was added in a single dose to start reactions or H_2O_2 was produced in situ by oxidation of glucose by GOx or by oxidation of formate by FOx. Reactions contained CFEs of catalase-deficient *E. coli* (0.1 g wet weight mL^{-1}) or a corresponding concentration (based on CO difference spectra) of purified protein, substrate (10 mM), acetone (5% [v/v]), H_2O_2 (20 mM) or GOx (0.2 U mL^{-1}) with glucose (100 mM) or FOx (0.2 U mL^{-1}) with formate (100 mM). Standard deviations of TONs were calculated using standard deviations of the product concentrations and the catalyst concentrations.

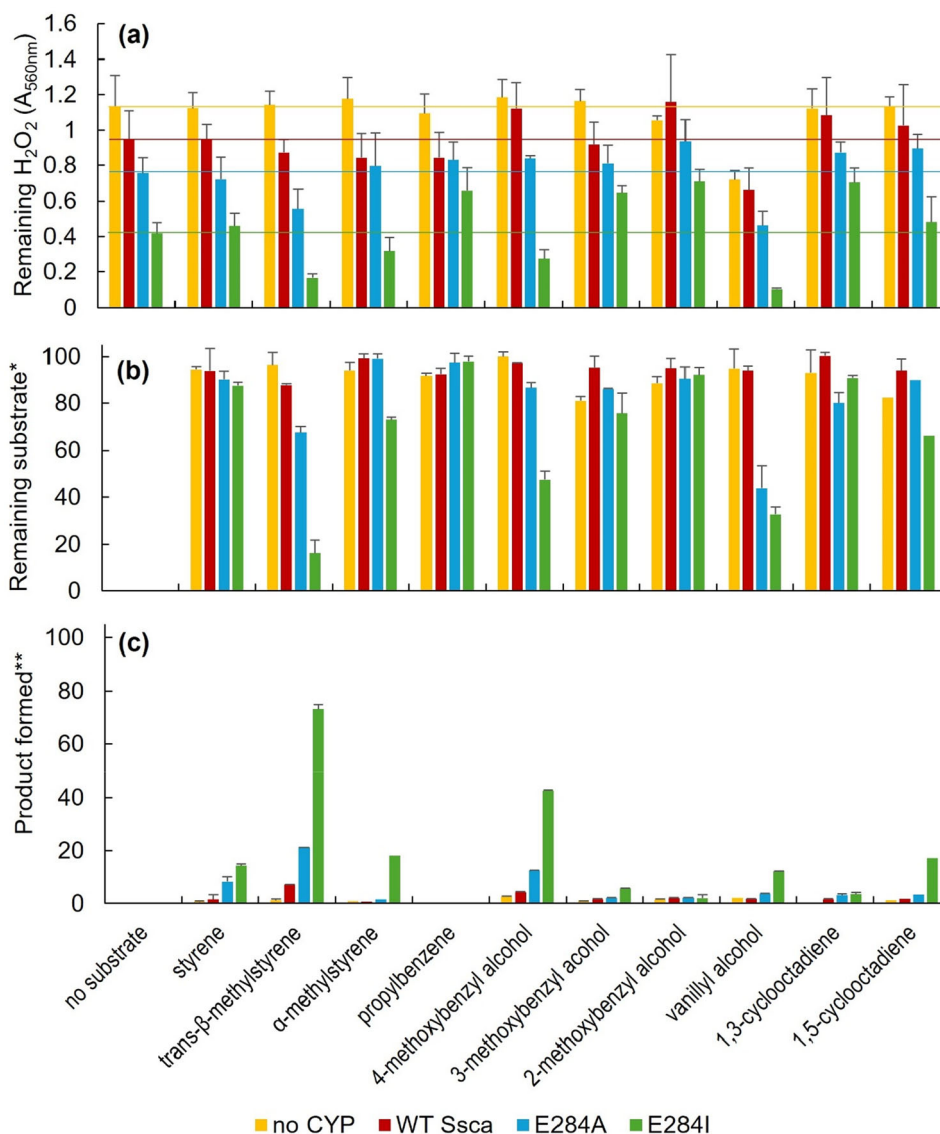


FIGURE 4 | (a) Remaining H_2O_2 (measured as absorbance at A_{560nm} in Ampliflu assay), (b) percentage remaining substrate, and (c) percentage product formed in reactions of WT *Ssca*CYP and its E284A and E284I mutants with 10 different substrates. Reactions (1 mL) contained WCs of catalase-deficient *E. coli* (0.1 g wet weight mL^{-1}), substrate (10 mM), acetone (5% [v/v]) and H_2O_2 (20 mM). H_2O_2 was added in a single dose to start reactions and assays and extractions were done after 4 h. The percentage remaining substrate and percentage product formed were calculated as percentage of maximum ratio of given substrate to internal standard in GC-FID assays. The percentage substrate and product are for reactions done in duplicate with Ampliflu assay for each reaction also done in duplicate.

alcohol, 2-methoxybenzyl alcohol, and 1,3-cyclooctadiene reduced H_2O_2 consumption by between 34% and 40%. On the other hand, with vanillyl alcohol residual H_2O_2 was markedly reduced even in the absence of enzyme. Although it is possible that H_2O_2 might directly react with a phenolic compound such as vanillyl alcohol, no product was detected in the GC analyses of the no-CYP control samples. It is more likely that this is an apparent reduction in H_2O_2 since interference of phenolic compounds with the Ampliflu Red assay has been described (Tama et al. 2023). The effects of enzymes and substrates on H_2O_2 consumption might explain why H_2O_2 consumption is not always suitable for detecting low activity levels. It might also explain why 20 variants selected by Xu et al. (2020) out of 8000 clones in their high-throughput screening based on H_2O_2 consumption, did not as purified enzymes display dramatically improved activity over the parental OleT_{JE} (CYP152L1) and CYP-

Sm46Δ29 (CYP152L2). High-throughput screening of peroxygenase libraries need not depend solely on H_2O_2 consumption, and the use of catalase-deficient WCs or CFEs can facilitate the development of complementary high-throughput screening methods for discovering improved or novel peroxygenases.

Finally, we used the conversion of *trans*- β -methylstyrene to cinnamaldehyde via cinnamyl alcohol by *Ssca*CYP_E284I to explore the use of catalase-deficient WCs in a preparative scale reaction. In this reaction, the biomass concentration was increased to 20 g wet weight mL^{-1} , and H_2O_2 was added in 10 mM aliquots every 4 h up to 12 h and then at 24 h. H_2O_2 accumulation, CYP stability (CO-difference spectra) and product formation was followed over 28 h at which time the total reaction mixture was extracted (Figure 5). Although the

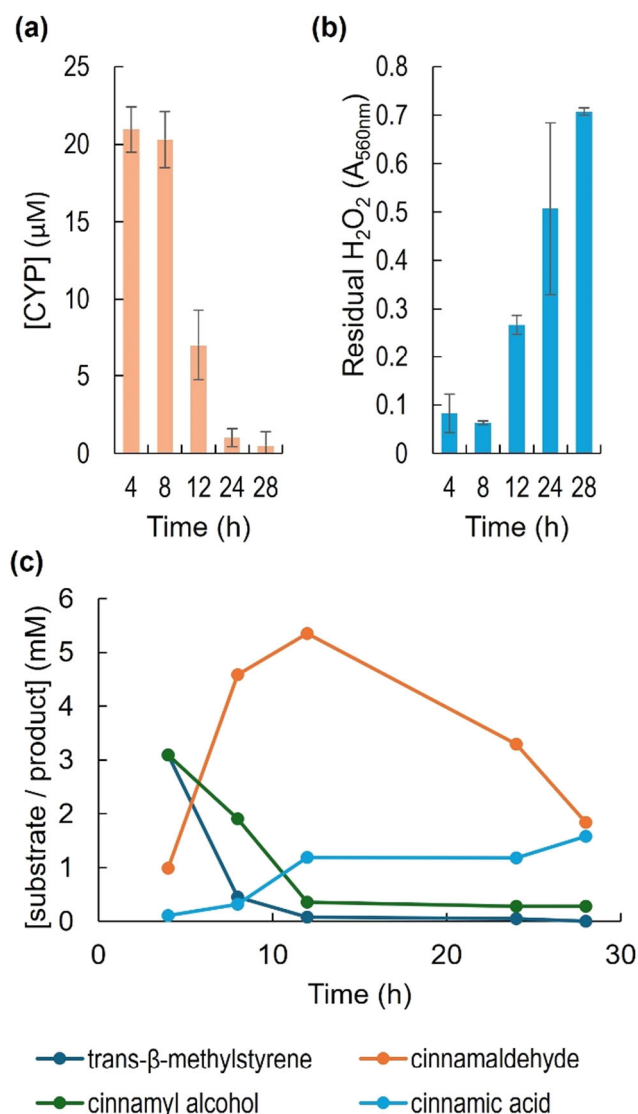


FIGURE 5 | Results from preparative scale conversion of *trans*-β-methylstyrene by the *SscaCYP_E284I* mutant. The reaction mixture (50 mL) contained WCs of catalase-deficient *E. coli* (0.2 g wet weight mL⁻¹), initial (CYP) 25 μM, substrate (10 mM) and acetone (5% [v/v]). The reaction was started by the addition of H₂O₂ (10 mM) with subsequent additions every 4 h (up to 12 h, and then at 24 h). Samples were taken every 4 h (up to 12 h, then at 24 and 28 h) to analyze enzyme stability (CO-difference spectra) (a), H₂O₂ accumulation (Ampliflu assay) (b) and *trans*-β-methylstyrene conversion (GC-FID) (c) with the total reaction mixture extracted after 28 h.

trans-β-methylstyrene was essentially completely (99%) converted after 12 h, we allowed the reaction to proceed for 28 h to obtain complete conversion of cinnamyl alcohol to cinnamaldehyde. This unfortunately led to significant oxidation of the cinnamaldehyde to cinnamic acid. Additionally, cinnamaldehyde could have been epoxidized and then oxidized to benzaldehyde by the H₂O₂ (Chen et al. 2012). Traces of benzaldehyde were detected in the final extracts (Figure S11). The eventual poor recovery of cinnamaldehyde (only 18%) might also be ascribed to Schiff base adduct formation of cinnamaldehyde in the amino acid-rich environment of the WCs (Wei et al. 2011). Further experiments will be required to determine the role residual H₂O₂ and WCs played in the loss of

cinnamaldehyde and to optimize reaction conditions and product recovery. However, our experiment demonstrates that catalase-deficient WCs are suitable for a preparative scale reaction in which over 5 mM cinnamaldehyde was formed after 12 h of reaction (Figure 5c).

The Arnold group employed a spectrophotometric assay in 96-well microtiter plates using clarified CFEs from mutant libraries expressed in catalase-deficient *E. coli* K-12 to screen for H₂O₂-driven hydroxylase activity (Cirino and Arnold 2003). It is surprising that there were no further reports on the use of such catalase-deficient *E. coli* strains in peroxygenase research until 2020 when Xu et al. for the first time reported using CFEs of a catalase deficient derivative of the commercially available, commonly used B strains in a H₂O₂ dependent high throughput screening for improved variants of CYP152 decarboxylases. Although it is possible, as demonstrated by Yan et al. (2024), to use WCs or CFEs of catalase-containing *E. coli* to screen large numbers of UPO variants for an improved characteristic, our results show that when activities are low, and specifically in the case of CYP peroxygenases, the use of catalase-deficient *E. coli* will be advantageous. We have demonstrated that peroxygenase containing WCs or CFEs from catalase-deficient *E. coli* generally perform as well as purified peroxygenases and that not only CFEs but also WCs of catalase-deficient *E. coli* can be used when screening for improved peroxygenases. However, it should be kept in mind that H₂O₂ is a very potent oxidizing agent which might react with the enzyme of interest destroying it or react directly with the substrate or products. Additionally, substrates or even products might interfere with H₂O₂ assays such as the peroxidase-dependent Ampliflu or Amplex Red assays. Thus, for both screening and preparative scale reactions extensive controls and optimization will be required for every enzyme-substrate combination whether purified peroxygenase, CFEs, or WCs are used.

3 | Materials and Methods

3.1 | Deletion of *katE* and *katG* in *E. coli* BL21-Gold(DE3)

CRISPR/Cas-assisted λ-red recombineering was used to create in-frame gene deletions. The start codon and the codons encoding the six residues of the C-terminus as well as the stop codon were left as described by Baba et al. (2006) for the construction of the Keio Collection.

The genome sequence of *E. coli* BL21(DE3) was used as a reference genome (GenBank accession number CP001509.3). Plasmids pEcCas (Addgene plasmid #73227) (Li et al. 2021) and pgRNA-bacteria (Addgene plasmid #44251) (Qi et al. 2013) were obtained from Addgene. The CRISPR/Cas-assisted λ-red recombineering was carried out as described before (Luelf et al. 2023). Briefly, gRNA targeting sequences were designed using the CHOPCHOP web toolbox (Labun et al. 2019) and cloned into the pgRNA-bacteria plasmid. For construction of the repair template, homology arms of approx. 500 bp length were amplified from boiled cells and combined by fusion PCR. Electrocompetent cells of *E. coli* BL21-Gold(DE3) harboring pEcCas were transformed with modified pgRNA and the repair

template as described in Supporting Information S1. The knockout was verified by colony PCR and sequencing (Eurofins Genomics, Germany). Curing of the plasmids pEcCas and pgRNA-bacteria was performed as described before (Lueft et al. 2023). Primers for amplification of the homology arms and exchange of the targeting sequence in the plasmid pgRNA are listed in Tables S1 and S2.

3.2 | Plasmids and Enzymes

For expression of the (CYP-)peroxygenases, the constructs pET-22b(+):CYP102A1_21B3, pET-28a(+):DcaUPO, pET-28a(+):SscaCYP_E284A, pET28a(+):SscaCYP and pET-28a(+):SscaCYP_E284I were obtained as described elsewhere (Aschenbrenner et al. 2024; Ebrecht et al. 2023; Ebrecht et al. 2023). The construct pET-21c(+):AoFOx for expression of the formate oxidase (FOx) from *Aspergillus oryzae* was kindly provided by Prof. Frank Hollmann (Delft University of Technology, the Netherlands) with permission of Prof. Andreas Bommarius (Georgia Institute of Technology, USA) (Tieves et al. 2019; Willot et al. 2020). All constructs were introduced into *E. coli* BL21-Gold(DE3) (WT) and the catalase-deficient strain *E. coli* BL21-Gold(DE3) $\Delta katE \Delta katG$ (CD). Heterologous expression and protein purification are described in the Supporting Information S1. GOx from *Aspergillus niger* was purchased from Sigma-Aldrich.

Concentrations of CYP peroxygenases were calculated using the usual extinction coefficient at 450 nm of $91 \text{ mM}^{-1} \text{ cm}^{-1}$ from the respective CO-difference spectra recorded using a Spectra-max M2 Microtiter Plate Reader (Molecular Devices Corporation) (Omura and Sato 1964, Guengerich et al. 2009). For DcaUPO, concentrations of purified protein were determined using the Pierce BCA assay kit (ThermoFisher Scientific), with bovine serum albumin as a standard. Purified DcaUPO was then used to calculate a concentration factor to determine the final concentration of enzyme in the CFEs and WCs from CO-difference spectra (at 450 nm).

3.3 | H₂O₂ Measurement

H₂O₂ stability was tested in WCs and CFES from wild-type and catalase-deficient *E. coli* (0.1 g wet weight mL^{-1}) in 200 mM potassium phosphate buffer pH 7.0. Reactions containing 800 μL of WCs or CFES and 10 mM of H₂O₂ were incubated at 25°C. Samples were taken at different time points and H₂O₂ concentrations were quantified with the Ampliflu Red assay (Sigma-Aldrich) (560 nm $\epsilon = 71\,000 \text{ M}^{-1} \text{ cm}^{-1}$) using the Spectramax M2 spectrophotometer.

3.4 | Biotransformations

Biotransformations were performed in 4 mL glass vials, in a final reaction volume of 1 mL. Reactions were incubated at 25°C with shaking at 200 rpm.

Reaction mixtures consisted of 800 μL of WCs or CFES from wild-type and catalase-deficient *E. coli* (0.1 g wet weight mL^{-1})

in 200 mM potassium phosphate buffer pH 7.0, 10 mM substrate, 5% (v/v) acetone, 20 mM H₂O₂ or 0.2 U GOx or FOx, 100 mM glucose or sodium formate. In reactions with purified proteins WCs or CFES were replaced with 800 μL 200 mM potassium phosphate buffer pH 7.0 containing purified peroxygenases at similar concentrations.

Reactions were stopped and extracted by addition of 1 mL ethyl acetate containing 2 mM internal standard (1-undecanol). Samples were analyzed by GC-FID (Shimadzu GC-2010) and GC-MS (Thermo Scientific TraceGC ultra—Trace DSQ) (Figures S2–S6) using a FactorFour VF-5ms column (60 m \times 0.32 mm \times 0.25 μm , Varian) column. Temperature program: 100°C hold 1 min, then 8°C min^{-1} up to 200°C. Concentrations of products and remaining substrates were calculated from standard curves of commercial standards and corrected for low levels of H₂O₂ oxidation in the absence of enzyme detected with cells transformed with empty plasmid. Chiral analysis of extracts from thioanisole reactions was performed by GC-FID (Thermo Scientific TraceGC ultra) using a CHIRALDEX B-TA column (30 m \times 0.25 mm \times 0.12 μm). Temperature program: 100°C hold 1 min then 1.5°C min^{-1} up to 136°C.

Averages and standard deviations were calculated from at least three independent reactions. Standard deviations of TONs were calculated using standard deviations of the product concentrations and the catalyst concentrations.

3.5 | Screening Experiment

Reactions for the screening experiment were performed as described above using WCs of catalase-deficient *E. coli* (0.1 g wet weight mL^{-1}) containing no CYP, SscaCYP (4 μM), SscaCYP_E284A (8 μM) and SscaCYP_E284I (8 μM). After 4 h 10 μL aliquots from each reaction mixture were transferred in duplicate to a 96-well microtiter plate and diluted 200 times in 200 mM potassium phosphate buffer pH 7.0. Remaining H₂O₂ levels were measured at 560 nm using the Ampliflu Red assay. The remaining reaction mixtures were extracted as described above and analyzed with GC-MS/FID (Thermo Scientific TraceGC ultra—Trace DSQ) (Figures S9 and S10) using the FactorFour VF-5ms column (60 m \times 0.32 mm \times 0.25 μm , Varian) column.

3.6 | Preparative Scale Reaction

A WC suspension (50 mL) of catalase-deficient *E. coli* (0.2 g wet weight mL^{-1} in 200 mM potassium phosphate buffer pH 7.0) containing SscaCYP E284I (ca. 20 μM) was supplemented with *trans*- β -methyl styrene (10 mM, 5% v/v acetone). The reaction was started by the addition of H₂O₂ (10 mM) and then incubated at 25°C with shaking at 200 rpm. Samples were taken every 4 h up to 12 h and then at 24 h. Enzyme stability (CO-difference spectra), H₂O₂ accumulation (quantification by Ampliflu Red assay), and substrate conversion (GC-MS/FID) (Figure S10) were evaluated, followed by the addition of H₂O₂ (10 mM). After 28 h enzyme, stability and H₂O₂ accumulation were evaluated and then the total reaction mixture was extracted with an equal volume of ethyl acetate.

Author Contributions

Martha Smit, Diederik J. Opperman, and Vlada B. Urlacher conceptualized the study and contributed to the design of experiments. Joost Luelf created the catalase-deficient *E. coli* strain. Ana C. Ebrecht designed and conducted most of the biotransformation experiments and analyzed the data. Kamini Govender performed the first biotransformation experiment with the catalase-deficient strain. Martha S. Smit prepared the first draft, and all authors then edited the manuscript. All authors approved the manuscript.

Acknowledgments

This work was supported by the South African Council for Scientific and Industrial Research—Industrial Biocatalysis Hub (CSIR-IBH) initiative funded by the South African Department of Science and Innovation (DSI) and the Technology Innovation Agency (TIA). We also thank Sarel Marais for technical assistance with GC analyses.

Ethics Statement

The authors have nothing to report.

Conflicts of Interest

The authors declare no conflicts of interest.

Data Availability Statement

The data that support the findings of this study are available from the corresponding author upon reasonable request.

References

- Aschenbrenner, J. C., A. C. Ebrecht, M. S. Smit, and D. J. Opperman. 2024. "Revisiting Strategies and Their Combinatorial Effect for Introducing Peroxygenase Activity in CYP102A1 (P450BM3)." *Molecular Catalysis* 557, no. February: 113953. <https://doi.org/10.1016/j.mcat.2024.113953>.
- Baba, T., T. Ara, M. Hasegawa, et al. 2006. "Construction of *Escherichia coli* K-12 in-Frame, Single-Gene Knockout Mutants: The Keio Collection." *Molecular Systems Biology* 2: 2006.0008. <https://doi.org/10.1038/msb4100050>.
- Chen, H. Y., Z. J. Yang, X. T. Zhou, and H. B. Ji. 2012. "Oxidative Cleavage of C=C Bond of Cinnamaldehyde to Benzaldehyde in the Presence of β -Cyclodextrin Under Mild Conditions." *Supramolecular Chemistry* 24, no. 4: 247–254. <https://doi.org/10.1080/10610278.2012.655277>.
- Cirino, P. C., and F. H. Arnold. 2002. "Regioselectivity and Activity of Cytochrome P450 BM-3 and Mutant F87A in Reactions Driven by Hydrogen Peroxide." *Advanced Synthesis & Catalysis* 344, no. 9: 932–937. [https://doi.org/10.1002/1615-4169\(200210\)344:9<932::AID-ADSC932>3.0.CO;2-M](https://doi.org/10.1002/1615-4169(200210)344:9<932::AID-ADSC932>3.0.CO;2-M).
- Cirino, P. C., and F. H. Arnold. 2003. "A Self-Sufficient Peroxide-Driven Hydroxylation Biocatalyst." *Angewandte Chemie International Edition* 42, no. 28: 3299–3301. <https://doi.org/10.1002/anie.200351434>.
- Ebrecht, A. C., T. M. Mofokeng, F. Hollmann, M. S. Smit, and D. J. Opperman. 2023. "Lactones From Unspecific Peroxygenase-Catalyzed in-Chain Hydroxylation of Saturated Fatty Acids." *Organic Letters* 25, no. 27: 4990–4995. <https://doi.org/10.1021/acs.orglett.3c01601>.
- Ebrecht, A. C., M. S. Smit, and D. J. Opperman. 2023. "Natural Alternative Heme-Environments Allow Efficient Peroxygenase Activity by Cytochrome P450 Monooxygenases." *Catalysis Science & Technology* 13, no. 21: 6264–6273. <https://doi.org/10.1039/d3cy01207g>.

- Guengerich, F. P., M. V. Martin, C. D. Sohl, and Q. Cheng. 2009. "Measurement of Cytochrome P450 and NADPH-Cytochrome P450 Reductase." *Nature Protocols* 4, no. 9: 1245–1251. <https://doi.org/10.1038/nprot.2009.121>.
- Hui, D., S. Khaiat, T. Uy, and H. Xu. 2014. "Partial Confirmation of Single *katG* and *katE* Knockouts and Double *katG/katE* Knockouts Created From Isogenic Background of *Escherichia coli* K-12 Strains." *Journal of Experimental Microbiology and Immunology (JEMI)* 18, no. April: 139–145.
- Kinner, A., K. Rosenthal, and S. Lütz. 2021. "Identification and Expression of New Unspecific Peroxygenases—Recent Advances, Challenges and Opportunities." *Frontiers in Bioengineering and Biotechnology* 9: 705630. <https://doi.org/10.3389/fbioe.2021.705630>.
- Labun, K., T. G. Montague, M. Krause, Y. N. Torres Cleuren, H. Tjeldnes, and E. Valen. 2019. "CHOPCHOP v3: Expanding the CRISPR Web Toolbox Beyond Genome Editing." *Nucleic Acids Research* 47, no. W1: W171–W174. <https://doi.org/10.1093/nar/gkz365>.
- Li, Q., B. Sun, J. Chen, Y. Zhang, Y. Jiang, and S. Yang. 2021. "A Modified pCas/pTargetF System for CRISPR-Cas9-Assisted Genome Editing in *Escherichia coli*." *Acta Biochimica et Biophysica Sinica* 53, no. 5: 620–627. <https://doi.org/10.1093/abbs/gmab036>.
- Linde, D., A. Olmedo, A. González-Benjumea, et al. 2020. "Two New Unspecific Peroxygenases From Heterologous Expression of Fungal Genes in *Escherichia coli*." *Applied and Environmental Microbiology* 86, no. 7: e02899-19. <https://doi.org/10.1128/AEM.02899-19>.
- Liu, F., R. Min, J. Hong, G. Cheng, Y. Zhang, and Y. Deng. 2021. "Quantitative Proteomic Analysis of ahpC/F and *katE* and *katG* Knockout *Escherichia coli*—A Useful Model to Study Endogenous Oxidative Stress." *Applied Microbiology and Biotechnology* 105, no. 6: 2399–2410. <https://doi.org/10.1007/s00253-021-11169-2>.
- Luelf, U. J., L. M. Böhmer, S. Li, and V. B. Urlacher. 2023. "Effect of Chromosomal Integration on Catalytic Performance of a Multi-Component P450 System in *Escherichia coli*." *Biotechnology and Bioengineering* 120, no. 7: 1762–1772. <https://doi.org/10.1002/bit.28404>.
- Monterrey, D. T., A. Menés-Rubio, M. Keser, D. Gonzalez-Perez, and M. Alcalde. 2023. "Unspecific Peroxygenases: The Pot of Gold at the End of the Oxyfunctionalization Rainbow?" *Current Opinion in Green and Sustainable Chemistry* 41: 100786. <https://doi.org/10.1016/j.cogsc.2023.100786>.
- Nakagawa, S., S. Ishino, and S. Teshiba. 1996. "Construction of Catalase Deficient *Escherichia coli* Strains for the Production of Uricase." *Bioscience, Biotechnology, and Biochemistry* 60, no. 3: 415–420. <https://doi.org/10.1271/bbb.60.415>.
- Omura, T., and R. Sato. 1964. "The Carbon Monoxide-Binding Pigment of Liver Microsomes." *Journal of Biological Chemistry* 239, no. 7: 2370–2378.
- Qi, L. S., M. H. Larson, L. A. Gilbert, et al. 2013. "Repurposing CRISPR as an RNA-Guided Platform for Sequence-Specific Control of Gene Expression." *Cell* 152, no. 5: 1173–1183. <https://doi.org/10.1016/j.cell.2013.02.022>.
- Salazar, O., P. C. Cirino, and F. H. Arnold. 2003. "Thermostabilization of a Cytochrome P450 Peroxygenase." *ChemBioChem* 4, no. 9: 891–893. <https://doi.org/10.1002/cbic.200300660>.
- Tama, A., G. Bartosz, and I. Sadowska-Bartos. 2023. "Phenolic Compounds Interfere in the Ampliflu Red/Peroxidase Assay for Hydrogen Peroxide." *Food Chemistry* 422, no. April: 136222. <https://doi.org/10.1016/j.foodchem.2023.136222>.
- Tieves, F., S. J. P. Willot, M. M. C. H. van Schie, et al. 2019. "Formate Oxidase (FOx) From *Aspergillus oryzae*: One Catalyst Enables Diverse H₂O₂-Dependent Biocatalytic Oxidation Reactions." *Angewandte Chemie International Edition* 58, no. 23: 7873–7877. <https://doi.org/10.1002/anie.201902380>.
- Wei, Q. Y., J. J. Xiong, H. Jiang, C. Zhang, and Ye Wen Ye. 2011. "The Antimicrobial Activities of the Cinnamaldehyde Adducts With Amino

Acids.” *International Journal of Food Microbiology* 150, no. 2–3: 164–170. <https://doi.org/10.1016/j.ijfoodmicro.2011.07.034>.

Willot, S. J. P., M. D. Hoang, C. E. Paul, et al. 2020. “FOx News: Towards Methanol-Driven Biocatalytic Oxyfunctionalisation Reactions.” *ChemCatChem* 12, no. 10: 2713–2716. <https://doi.org/10.1002/cctc.202000197>.

Xu, H., W. Liang, L. Ning, et al. 2020. “Directed Evolution of P450 Fatty Acid Decarboxylases Via High-Throughput Screening Towards Improved Catalytic Activity.” *ChemCatChem* 12, no. 1: 80–84. <https://doi.org/10.1002/cctc.201901347>.

Xu, X., T. Hilberath, and F. Hollmann. 2023. “Selective Oxyfunctionalisation Reactions Catalysed by P450 Monooxygenases and Peroxygenases—A Bright Future for Sustainable Chemical Synthesis.” *Current Opinion in Green and Sustainable Chemistry* 39: 100745. <https://doi.org/10.1016/j.cogsc.2022.100745>.

Yan, X., X. Zhang, H. Li, et al. 2024. “Engineering of Unspecific Peroxygenases Using a Superfolder-Green-Fluorescent-Protein-Mediated Secretion System in *Escherichia coli*.” *JACS Au* 4, no. 4: 1654–1663. <https://doi.org/10.1021/jacsau.4c00129>.

Supporting Information

Additional supporting information can be found online in the Supporting Information section.